

Electrical properties of GaN/poly(3-hexylthiophene) interfaces

B.-N. Park,^{1,a)} J. J. Uhlrich,² T. F. Kuech,² and P. G. Evans^{1,b)}

¹Materials Science and Engineering, University of Wisconsin, Madison, Wisconsin 53706, USA

²Chemical and Biological Engineering, University of Wisconsin, Madison, Wisconsin 53706, USA

(Received 8 April 2009; accepted 3 June 2009; published online 10 July 2009)

Interfaces between wide-bandgap semiconductors and polymeric electronic materials are model systems for geometrically more complicated interfaces formed in nanostructured composite electronic, photonic, and photovoltaic devices. The wide-bandgap semiconductor GaN is readily available with well-defined electronic and structural properties, including reproducible control of doping and conductivity type, and can ideally serve as the inorganic side of the model system. Electron transport through a GaN/poly(3-hexylthiophene) (P3HT) semiconductor heterojunction depends on the conductivity type of the GaN and on the doping level in the polymer. The total contact resistance of a planar P3HT film with GaN contacts in a symmetric *p*-GaN/P3HT/*p*-GaN structure is consistent with the contribution of reversed-biased junction at one of the GaN/P3HT interfaces. An *n*-GaN/P3HT/*n*-GaN structure has a lower total resistance than the *p*-GaN structure, possibly arising from band-to-band tunneling at the interface. Doping the P3HT layer with iodine greatly reduced the contact resistance for interfaces with both conductivity types of GaN. © 2009 American Institute of Physics. [DOI: 10.1063/1.3159653]

I. INTRODUCTION

Composite electronic materials with both organic and inorganic constituents are valuable components of emerging photovoltaics, transistors, light emitters, and sensors.¹⁻⁴ These devices rely on the interfaces between organic semiconductors and inorganic electrodes to separate and to transport charge. Interfaces in photovoltaics for solar applications, for example, can include wide-bandgap semiconductors such as ZnO or TiO₂ and organic semiconductors such as poly(3-hexylthiophene) (P3HT).⁵ P3HT is particularly valuable as a model organic semiconductor because it has been widely studied as both an electronic and optoelectronic material.⁶ It has been difficult in the past to probe the molecular-scale origins of the electronic properties of interfaces between organic semiconductors and nanoparticles of wide-bandgap inorganic semiconductors because it is not yet possible to vary the electronic properties of the inorganic nanoparticles precisely. In comparison, elemental metal contacts to organic semiconductors have been studied under a range of processing conditions, leading to both fundamental and practically useful results.⁷⁻⁹ Metals, however, do not present the degree of electronic tunability or utility in composite devices of wide-bandgap semiconductors.

The potential to synthesize inorganic semiconductors reproducibly with a wide range of electronic properties allows experiments to explore the full range of possible band alignments and transport processes, including thermally activated and tunneling phenomena. Here, we describe the electronic properties of a model system consisting of an interface between P3HT and thin films of the wide-bandgap semiconductor GaN. The mechanisms of charge transport available at

metal-organic and semiconductor-organic interfaces include thermal activation over a barrier,¹⁰ field-assisted tunneling,¹¹ and band-to-band tunneling.¹²⁻¹⁴ We show that a Schottky barrier description applies to the P3HT interface with *p*-type GaN, and a tunneling mechanism may be involved at the interface between P3HT and *n*-type GaN.

GaN can be functionalized with molecular layers including organic optical and electronic materials and biomolecules through a variety of chemical and photochemical processes.¹⁵⁻¹⁹ These strategies promise to allow the organic side of the GaN/organic semiconductor interface to be reproducibly varied by adding electronically active functional groups. Chemically and electronically functionalized interfaces with GaN can be designed on the basis of straightforward concepts because GaN has surface properties conducive to the formation of heterojunctions with organic materials that can be described with electrical models derived from inorganic heterostructures.²⁰ The band alignments at interfaces in inorganic semiconductor heterostructures can be derived from the atomic structure of the interface.²¹ A similar precision is beginning to emerge in organic/inorganic material systems.

There is no substantial pinning of the Fermi level by surface states at GaN surfaces.^{22,23} Organic/inorganic heterojunctions, however, can form significant interface dipoles in some cases,²⁴⁻²⁶ including experiments that suggest that charge is injected from levels with energy levels far deeper than the highest occupied molecular orbital (HOMO).²⁷ The energy levels relevant for these effects can arise within the organic semiconductor as well as from states at the inorganic semiconductor surface. It thus cannot necessarily be assumed, without further evidence, that the GaN/organic semiconductor interface is completely free of Fermi level pinning.

Despite the potential for the formation of interface dipoles and states residing in the organic layer, the GaN/

^{a)}Present address: Georgia Institute of Technology, School of Chemical and Biomolecular Engineering, 311 Ferst Drive, N.W., Atlanta, GA 30332-0100.

^{b)}Electronic mail: evans@engr.wisc.edu.

pentacene interface showed negligible interface dipole formation.²⁸ The similarity between the electronic structure of pentacene and other organic semiconductors suggests that the band alignments at interfaces between GaN and organic semiconductors, in general, can be described using the differences between their equilibrium band structures. We will thus use the Schottky–Mott model to predict the electronic properties of interfaces between GaN and organic semiconductors and point out its potential limitations in this system.¹⁰

Interfaces between organic and inorganic semiconductors are unlike metal/organic semiconductor contacts in that these semiconductor heterojunctions have properties that can be tuned on both sides of the interface. In addition, wide-bandgap semiconductors, including GaN and other materials such as ZnO, possess valence bands that are deep with respect to the vacuum, potentially facilitating hole transport from the inorganic semiconductor to the organic semiconductor.

II. GAN/THIOPHENE INTERFACE FORMATION AND CHARACTERIZATION

Electrical contacts to P3HT thin films were formed using GaN heteroepitaxial layers on Al₂O₃ substrates. Two distinct sets of samples were used to determine the effect of the conductivity type of the GaN layer on the electrical properties of the GaN/P3HT interface. Separate contact structures were formed using *n*- and *p*-type GaN thin films as starting points. The *n*-type GaN layers had a thickness of 5 μm, grown using hydride vapor phase epitaxy (HVPE) on (0001)-oriented sapphire and doped with Si to an electron concentration of approximately 1 × 10¹⁸ cm⁻³ at room temperature. The *p*-type GaN layers were grown by metal-organic vapor phase epitaxy to a thickness of 5 μm on a nominally undoped HVPE-grown layer and possessed a hole concentration of approximately 2 × 10¹⁸ cm⁻³. Ohmic contact metalizations on *p*-type GaN were formed using a Ni/Au structure annealed in air at 500 °C for 10 min, following a procedure that has been shown to result in low-resistance contacts.²⁹ The contacts to *n*-type GaN consisted of unannealed Ti/Al layers.^{30,31}

The GaN layers were patterned into the symmetric structures shown schematically in Fig. 1(a). Isolated GaN mesas were formed by first patterning a photoresist layer using photolithography and subsequently etching through the GaN layer to the sapphire substrate using electron cyclotron resonance plasma etching with a Cl₂/H₂/Ar/CH₄ chemistry.³² P3HT films with a thickness of 250 ± 15 nm were deposited by spin coating at 1500 rpm using a solution of 25 mg of P3HT per 1 ml of chloroform solvent. The spin-coated P3HT film was patterned using acetone and a sharp paint brush to eliminate the effect of current between Ni/Au electrodes. The structures fabricated with *p*-GaN and *n*-GaN contacts were also compared to metal/P3HT contacts using metal layers consisting of 500 nm thick Au on a 10 nm thick Ni adhesion layer on a SiO₂-coated Si wafer.

The contact structures shown in Fig. 1 were used to make two-terminal current-voltage transmission line mea-

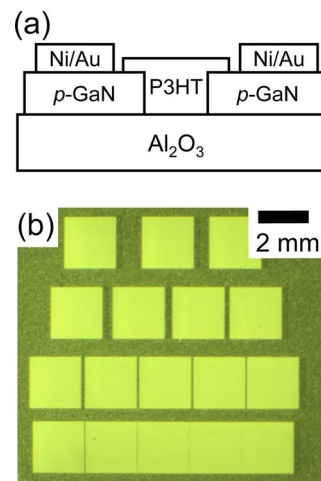


FIG. 1. (Color online) (a) Schematic cross section of the test structure for *p*-type GaN contacts to P3HT. (b) Optical micrograph of the patterned *p*-GaN layer before the formation of the metal and P3HT layers.

surements that were subsequently analyzed using the transfer length method.³³ The resistance of a resistor of length L in this geometry is

$$R_{\text{total}} = R_s \frac{L}{w} + R_c. \quad (1)$$

Here R_s is the sheet resistance of the thin film and R_c is the total resistance of both contacts. The contacts had widths w of 2 mm and separations L ranging from 5 μm to 1 mm, as shown in Fig. 1(b). The contact resistance extracted from the variation the total resistance as a function of the contact separation L using Eq. (1) is accurate only when the contacts are exactly Ohmic. Some aspects of the scaling of structures with non-Ohmic contacts can be recovered using a more detailed description of the processes of charge injection and transport.³⁴

The concentration of holes in P3HT can be altered by exposing thin films of P3HT to iodine.³⁵ After electrical measurements on undoped films, the P3HT layers were exposed to vapor from iodine heated to 30 °C in air on a hot plate beneath an inverted Petri dish. Dissolving the doped P3HT in a solvent and redepositing undoped P3HT onto the same GaN contact patterns yielded electrical properties consistent with undoped P3HT, indicating that the doping process did not appreciably modify the GaN.

III. RESULTS

Current-voltage characteristics obtained using *p*- and *n*-type GaN contacts to P3HT are shown in Figs. 2 and 3, respectively, for a number of spacings between the GaN contacts. The *p*-GaN contacts (Fig. 2) produced lower currents than *n*-GaN contacts (Fig. 3) and exhibited highly nonlinear current-voltage characteristics. The current was fitted to a linear function of the voltage the range between -1 and 1 V to obtain the low-bias resistance for each spacing of the contacts. The resistances obtained in this way are plotted in Fig. 4. The P3HT sheet resistances obtained by applying Eq. (1) to the data in Fig. 4 were 1.8 × 10⁸ Ω/□ with *p*-GaN con-

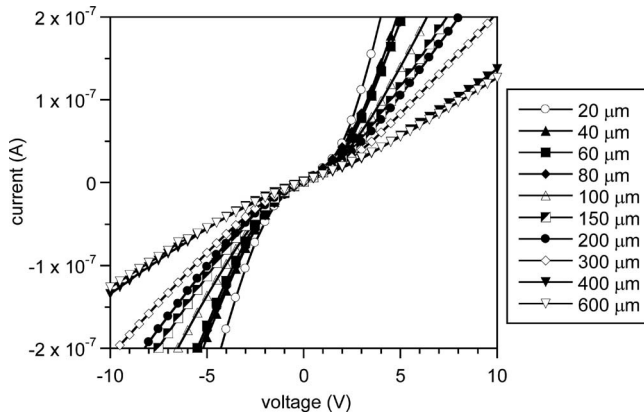


FIG. 2. Current-voltage characteristics for P3HT with *p*-GaN contacts with a variety of spacings.

tacts and $2.2 \times 10^8 \Omega/\square$ with *n*-GaN. The sheet resistance measured using Au/Ni contacts was $3.6 \times 10^8 \Omega/\square$.

The total contact resistances for contacts between P3HT and *n*-GaN, *p*-GaN, and Au/Ni were substantially different. With Au/Ni contacts, the contact resistance was $R_c = 2.7 \times 10^6 \Omega$ and the contact resistance-width product $R_c w$ was $6 \times 10^5 \Omega \text{ cm}$, somewhat larger than values obtained in previous studies of similar Au/P3HT contacts.³⁶ The total contact resistances with different GaN conductivity types were $1.1 \times 10^7 \Omega$ with *p*-GaN and $2.9 \times 10^6 \Omega$ with *n*-GaN. These electrical results are summarized in Table I.

Iodine-doped samples exhibited far lower total resistances than the undoped P3HT, as shown in the plot of resistance as a function of contact spacing in Fig. 5. The sheet resistance of iodine-doped P3HT was lower than the undoped material by approximately three orders of magnitude, with values of 2×10^5 and $7 \times 10^5 \Omega/\square$ for *p*-GaN and *n*-GaN contacts, respectively. The contact resistance dropped by similar factors to $2.8 \times 10^3 \Omega$ with *p*-GaN contacts and $7.7 \times 10^3 \Omega$ with *n*-GaN contacts. The sheet resistance of the P3HT sample with Au/Ni contacts decreased less to $2.8 \times 10^7 \Omega/\square$ with a contact resistance of $6.5 \times 10^5 \Omega$. The subtle differences between the iodine-doped P3HT layers with contacts formed from different conductivity types of GaN and Au/Ni could arise from variation in the iodine concentration from sample to sample and thus are difficult to interpret in terms of the electronic structure of the interface.

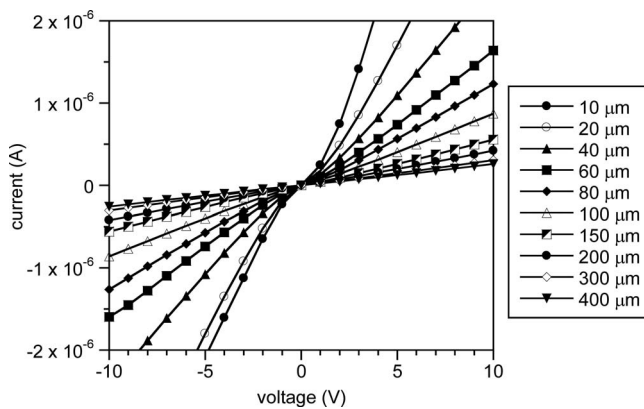


FIG. 3. Current-voltage characteristics for P3HT with *n*-GaN contacts.

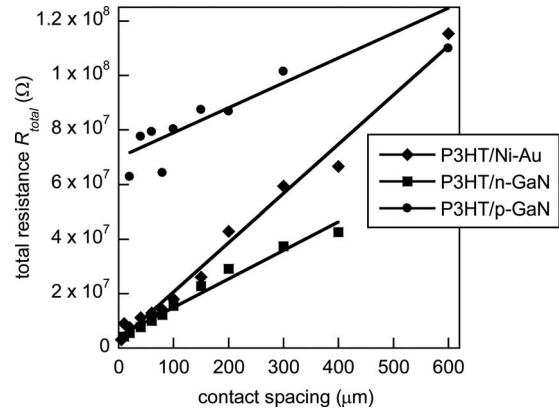


FIG. 4. Total resistance measured from the low voltage bias region of the current-voltage characteristics for P3HT with contacts formed from *p*-GaN (circles) and *n*-GaN (squares) epitaxial layers on Al_2O_3 and for P3HT films on SiO_2 with Au/Ni contacts (diamonds). The lines show the best linear fit to each series of resistances as a function of the contact spacing.

The absolute concentrations of mobile charge carriers and iodine species in the P3HT film were not characterized in this study. It is clear, however, that the iodine-doped P3HT samples do not form the highly resistive, reverse-biased contact observed with undoped P3HT.

IV. DISCUSSION

The current-voltage characteristics for electron transport across the P3HT/GaN heterojunction are largely determined by the band alignments at the interface.¹⁰ A comprehensive study of the band alignment at the P3HT/GaN interface is not yet available, but some insight can be gained from the values for the ionization potentials of GaN and P3HT. An *n*-GaN surface that has been exposed to ambient conditions has an ionization potential of 7.93 eV.^{28,37} P3HT has a much shallower ionization potential of 4.85 eV.³⁸ A schematic band alignment based on these values is shown in Fig. 6.

The schematic band alignment at the P3HT/GaN interface in Fig. 6 is similar to the interface between *n*-GaN and pentacene for which the band alignments have been previously determined.²⁸ P3HT and pentacene are both hole-transporting materials and have similar relevant molecular energy levels.^{28,39} Experimentally observed band alignments could also be influenced by interfacial dipoles or charged states within the bandgap. These effects have not been considered in Fig. 6.

In the absence of interfacial dipole moments or states in the bandgap, the band alignment shown in Fig. 6 favors the transport of holes from *p*-GaN into P3HT because the valence band of GaN is far deeper, by approximately 3 eV, than

TABLE I. Contact resistances for interfaces between undoped P3HT and *p*-GaN, *n*-GaN, and Au/Ni.

Contact	R_c (Ω)
<i>p</i> -GaN	1.1×10^7
<i>n</i> -GaN	2.9×10^6
Au/Ni	2.7×10^6

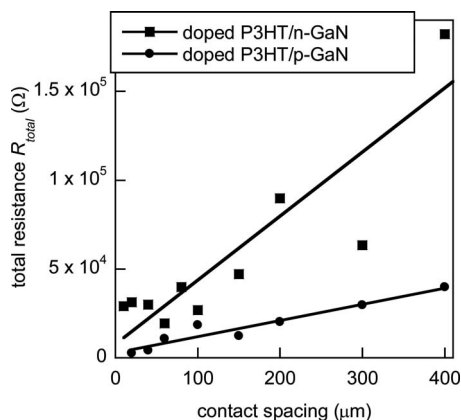


FIG. 5. Total resistance as a function of electrode spacing for iodine-doped P3HT with *p*-GaN (circles) and *n*-GaN (squares) contacts.

the HOMO of P3HT. This large energy difference, however, also makes the transport of holes from P3HT into *p*-GaN energetically unfavorable. The large contact resistance between P3HT and *p*-GaN thus arises from the large-barrier side of the GaN/P3HT/GaN structure becoming reverse biased. The large barrier for hole transport into *p*-GaN is also apparent in the nonlinearity of the current-voltage characteristics in Fig. 2. The Au/P3HT interface has a smaller contact resistance than the *p*-GaN/P3HT interface because hole transport from P3HT into Au faces a smaller barrier of less than 1 eV.³⁹

The comparatively low contact resistance when P3HT is contacted by *n*-type GaN is not consistent with thermally activated transport over the large energy barriers illustrated in Fig. 6. The band alignment predicted using the Schottky–Mott rule, shown in Fig. 6, however, favors a band-to-band tunneling mechanism allowing carriers to tunnel across the GaN/P3HT interface and producing far larger currents through the interface than would be expected from a Schottky model.^{12,13} The band alignment in Fig. 6 is based on the assumption that the Fermi level at the P3HT/GaN interfaces is unpinned. Under this assumption, tunneling between *n*-GaN and P3HT would be facilitated by the energetic alignment of occupied levels in the HOMO of P3HT with the conduction band of *n*-type GaN (Fig. 6). Tunneling is also influenced by the structural and electronic disorder on the organic side of the interface.⁴⁰ Disorder in the P3HT layer may thus allow tunneling despite the difference in orbital character between the GaN conduction band and the P3HT

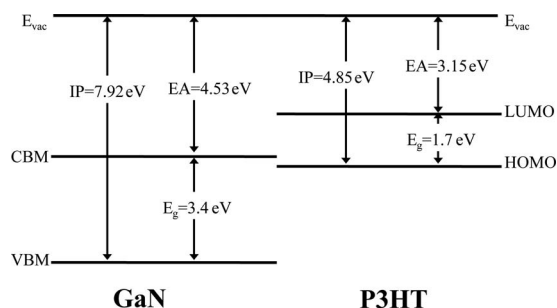


FIG. 6. Schematic band alignment at interfaces between GaN and P3HT. The vacuum level (E_{vac}), ionization potential (IP), electron affinity (EA), and bandgap (E_g) are indicated.

HOMO. A tunneling mechanism would result in the absence of a large contact resistance for injecting holes into P3HT from *n*-GaN. The occupied energy levels of *p*-GaN and P3HT are not aligned to facilitate tunneling and the removal of holes at from P3HT into GaN at *p*-GaN/P3HT interfaces thus occurs by thermal activation over the Schottky barrier.

V. CONCLUSION

The versatility of compound semiconductors in exploring the physics and chemistry of electronic contacts to organic semiconductors is just beginning to be exploited. We propose, for example, that the high resistance we observe here for the reverse-biased contact between *p*-type GaN and P3HT will have other electrical consequences. Hole injection from *p*-type GaN into P3HT would benefit from the large mismatch in the energy levels of *p*-GaN and organic semiconductors. Hole injecting contacts based on GaN and related *p*-type wide-bandgap semiconductors could offer new strategies for incorporating transparent conductors in organic electronics, for example, in the form of polycrystalline *p*-GaN.

The low contact resistance at interfaces between *n*-type GaN and P3HT shows that tunneling contacts between organic semiconductors and wide-bandgap inorganic semiconductors can be fabricated using *n*-type inorganic semiconductors. Promising avenues for further control of this effect include varying the bandgap of the nitride semiconductors via In/Ga/Al alloying to create quantum well structures with electronic states that are resonant with molecular energy levels. Further study of these interfaces with spectroscopic and potentiometric probes will provide the energetic information necessary to form a more complete picture of the relevant interface electronic transport properties.

ACKNOWLEDGMENTS

This work was supported by the University of Wisconsin Materials Research Science and Engineering Center (NSF Grant No. DMR-0520527). J. J. U. was supported by a graduate research fellowship from the National Science Foundation.

¹B. A. Gregg, *J. Phys. Chem. B* **107**, 4688 (2003).

²S. Coe, W. K. Woo, M. Bawendi, and V. Bulovic, *Nature (London)* **420**, 800 (2002).

³H. Nakanotani, M. Yahiro, C. Adachi, and K. Yano, *Appl. Phys. Lett.* **90**, 262104 (2007).

⁴P. T. Hammond, *Adv. Mater. (Weinheim, Ger.)* **16**, 1271 (2004).

⁵D. C. Olson, J. Piris, R. T. Collins, S. E. Shaheen, and D. S. Ginley, *Thin Solid Films* **496**, 26 (2006).

⁶H. Sirringhaus, P. J. Brown, R. H. Friend, M. M. Nielsen, K. Bechgaard, B. M. W. Langeveld-Voss, A. J. H. Spiering, R. A. J. Janssen, E. W. Meijer, P. Herwig, and D. M. de Leeuw, *Nature (London)* **401**, 685 (1999).

⁷M. Abkowitz, J. S. Facci, and J. Rehm, *J. Appl. Phys.* **83**, 2670 (1998).

⁸Y. L. Shen, A. R. Hosseini, M. H. Wong, and G. G. Malliaras, *ChemPhysChem* **5**, 16 (2004).

⁹B. H. Hamadani, D. A. Corley, J. W. Ciszek, J. M. Tour, and D. Natelson, *Nano Lett.* **6**, 1303 (2006).

¹⁰J. O. McCaldin, *Prog. Solid State Chem.* **26**, 241 (1998).

¹¹D. V. Khramtchenkov, H. Bassler, and V. I. Arkhipov, *J. Appl. Phys.* **79**, 9283 (1996).

¹²L. Esaki, *Phys. Rev.* **109**, 603 (1958).

¹³J. Appenzeller, Y. M. Lin, J. Knoch, and P. Avouris, *Phys. Rev. Lett.* **93**, 196805 (2004).

- ¹⁴J. S. Chen, L. L. Xu, J. Lin, Y. H. Geng, L. X. Wang, and D. G. Ma, *Appl. Phys. Lett.* **89**, 083514 (2006).
- ¹⁵H. Kim, P. E. Colavita, K. M. Metz, B. M. Nichols, B. Sun, J. Uhrlich, X. Y. Wang, T. F. Kuech, and R. J. Hamers, *Langmuir* **22**, 8121 (2006).
- ¹⁶H. Kim, P. E. Colavita, P. Paoprasert, P. Gopalan, T. F. Kuech, and R. J. Hamers, *Surf. Sci.* **602**, 2382 (2008).
- ¹⁷A. Arranz, C. Palacio, D. Garcia-Fresnadillo, G. Orellana, A. Navarro, and E. Munoz, *Langmuir* **24**, 8667 (2008).
- ¹⁸T. Ito, S. M. Forman, C. Cao, F. Li, C. R. Eddy, M. A. Mastro, R. T. Holm, R. L. Henry, K. L. Hohn, and J. H. Edgar, *Langmuir* **24**, 6630 (2008).
- ¹⁹E. Estephan, C. Larroque, F. J. G. Cuisinier, Z. Balint, and C. Gergely, *J. Phys. Chem. B* **112**, 8799 (2008).
- ²⁰L. Burgi, T. J. Richards, R. H. Friend, and H. Sirringhaus, *J. Appl. Phys.* **94**, 6129 (2003).
- ²¹W. R. Frensley and H. Kroemer, *Phys. Rev. B* **16**, 2642 (1977).
- ²²M. A. Reshchikov, S. Sabuktagin, D. K. Johnstone, and H. Morkoc, *J. Appl. Phys.* **96**, 2556 (2004).
- ²³S. Chevtchenko, X. Ni, Q. Fan, A. A. Baski, and H. Morkoc, *Appl. Phys. Lett.* **88**, 122104 (2006).
- ²⁴I. G. Hill, A. Rajagopal, A. Kahn, and Y. Hu, *Appl. Phys. Lett.* **73**, 662 (1998).
- ²⁵H. Ishii and K. Seki, *IEEE Trans. Electron Devices* **44**, 1295 (1997).
- ²⁶H. Ishii, K. Sugiyama, E. Ito, and K. Seki, *Adv. Mater. (Weinheim, Ger.)* **11**, 605 (1999).
- ²⁷C. Tengstedt, W. Osikowicz, W. R. Salaneck, I. D. Parker, C.-H. Hsu, and M. Fahlman, *Appl. Phys. Lett.* **88**, 053502 (2006).
- ²⁸J. Uhrlich, M. Garcia, S. Wolter, A. S. Brown, and T. F. Kuech, *J. Cryst. Growth* **300**, 204 (2007).
- ²⁹J.-K. Ho, C.-S. Jong, C. C. Chiu, C.-N. Huang, C.-Y. Chen, and K.-K. Shih, *Appl. Phys. Lett.* **74**, 1275 (1999).
- ³⁰N. A. Papanicolaou and K. Zekentes, *Solid-State Electron.* **46**, 1975 (2002).
- ³¹J. K. Kim, H. W. Jang, and J.-L. Lee, *J. Appl. Phys.* **91**, 9214 (2002).
- ³²J. Lee, H. Cho, D. C. Hays, C. R. Abernathy, S. J. Pearton, R. J. Shul, G. A. Vawter, and J. Han, *IEEE J. Sel. Top. Quantum Electron.* **4**, 557 (1998).
- ³³D. K. Schroder, *Semiconductor Material Device and Characterization* (Wiley-Interscience, Hoboken, NJ, 2006).
- ³⁴B. H. Hamadani and D. Natelson, *J. Appl. Phys.* **97**, 064508 (2005).
- ³⁵S. Ukai, H. Ito, K. Marumoto, and S. I. Kuroda, *J. Phys. Soc. Jpn.* **74**, 3314 (2005).
- ³⁶L. Burgi, H. Sirringhaus, and R. H. Friend, *Appl. Phys. Lett.* **80**, 2913 (2002).
- ³⁷J. E. Lyon, A. J. Cascio, M. M. Beerbom, R. Schlaf, Y. Zhu, and S. A. Jenekhe, *Appl. Phys. Lett.* **88**, 222109 (2006).
- ³⁸Y. Yi, J. E. Lyon, M. M. Beerbom, and R. Schlaf, *J. Appl. Phys.* **100**, 093719 (2006).
- ³⁹Y. D. Park, J. H. Cho, D. H. Kim, Y. Jang, H. S. Lee, K. Ihm, T.-H. Kang, and K. Cho, *Electrochem. Solid-State Lett.* **9**, G317 (2006).
- ⁴⁰J. C. Scott, *J. Vac. Sci. Technol. A* **21**, 521 (2003).